Preparation and Structure of a Quadruply-bonded Dimolybdenum Mixed Complex with Acetate and 7-Azaindole Ligands

FRANÇOIS ALLAIRE and ANDRÉ L. BEAUCHAMP*

Département de Chimie, Université de Montréal, C.P. 6128, Succ. A, Montréal, Qué., H3C 3J7, Canada

(Received July 6, 1988)

Abstract

By reacting $Mo_2(acetate)_4$ with 7-azaindole in the presence of Na methoxide in ethanol, the mixed complex $Mo_2(acetate)_2(7\text{-azaindolyl})_2$ was obtained. Recrystallization from DMF yielded monoclinic crystals of the 2DMF adduct: $P2_1/c$, $a = 8.378(2)$, $b = 9.166(2)$, $c = 17.387(4)$ Å, $\beta = 101.21(2)°$, $R = 0.039$. The dimer contains quadruply bonded Mo≣Mo units (2.1121(5) Å) surrounded by two bridging acetates and two bridging azaindole ligands alternating about the Mo–Mo axis. The two axial positions are occupied by the DMF molecules (Mo–O = 2.598(4) Å). The azaindole ligands are involved in a two-fold orientation disorder consistent with the presence of two isomeric forms in the crystal, which are detected by the presence of two signals for each azaindole resonance in the ^1H NMR spectrum of the DMF solution. The strong characteristic Mo≣Mo stretching vibration is observed at 377 cm^{-1} in the Raman spectrum.

Introduction

Compounds containing quadruple Mo≣Mo bonds are now known for many bridging ligands [1]. However, the vast majority of these ligands are either carboxylates or direct derivatives thereof, or *ortho*-substituted phenyl, pyridine or similar single ring units. Bridging ligands in which both donor atoms are part of more rigid two-ring systems have received little attention as yet. The crescent-shaped ligands with a central naphthyridine portion have apparently been used so far only for Rh–Rh compounds [2]. To our knowledge, the only Mo≣Mo complex with a ligand of this type is the $Mo_2Cl_2(PEt_3)_2(Aza)_2$ compound containing the monoanion (Aza^-) of 7-azaindole (**I**), studied by Cotton *et al.* [3].

In the present paper, we are reporting on a mixed complex $Mo_2(acetate)_2(Aza)_2$. No other dimeric units containing two bridging ligands structurally so different are known. Partial replacement of carboxylates in $Mo_2(carboxylate)_4$ compounds by pyrazolylborates, acetylacetonate or related moieties led to complexes in which these ligands are chelating, but not bridging [4]. A major question raised by the present compound was the ability of the 7-azaindole anion to bridge in the presence of acetate, in spite of the larger N1–N7 'bite' imposed by its five-membered ring.

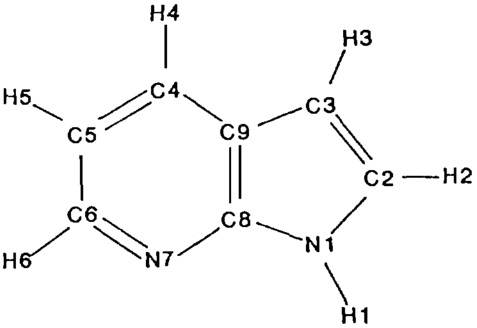

Experimental

Chemicals

$Mo_2(O_2CCH_3)_4$ was prepared from $Mo(CO)_6$ (Aldrich) by a known procedure [5].

7-Azaindole (Aldrich) was used without further purification. In order to obtain the N1-D derivative, the commercial product was dissolved in 40% $NaOD/D_2O$ and kept warm for 30 min. The volume was reduced by 50%, the mixture was allowed to cool to room temperature and filtered. ^1H NMR showed the sample to be fully deuterated at N1 and partially deuterated at C3. Complete deuteration at N1 and C3 was achieved by refluxing the latter sample in D_2O for 2 h.

Preparation of the Mo compounds was carried out under anaerobic conditions in dry degassed solvents using Schlenk glassware.

Preparation

$Mo_2(O_2CCH_3)_2(Aza)_2$

To 0.43 g (1.0 mmol) of $Mo_2(O_2CCH_3)_4$ in 40 ml of ethanol was added 0.47 g (4.0 mmol) of 7-azaindole and 0.22 g (4.0 mmol) of $NaOCH_3$.

---

*Author to whom correspondence should be addressed.

0020-1693/89/$3.50

This mixture was stirred under reflux for 18 h, during which time the mixture turned brown. After cooling to room temperature, the solid was filtered, washed with ethanol, and dried overnight under vacuum. This procedure gave 0.41 g (75%) of a light brown powder. *Anal.* Calc. for $C_{18}H_{16}Mo_2N_4O_4$: Mo, 35.4. Found (calcination to MoO_3 at 600 °C) [6]: 34.8%.

The same complex was also obtained by adding only 2 mmol of 7-azaindole and $NaOCH_3$ per mmol of $Mo_2(O_2CCH_3)_4$.

$Mo_2(O_2CCH_3)_2(Aza)_2 \cdot 2DMF$

The adduct was obtained by dissolving $Mo_2(O_2CCH_3)_2(Aza)_2$ in hot DMF. After standing at room temperature for several days, a few brown crystals appeared. They were filtered and dried gently under vacuum. These crystals were suitable for X-ray diffraction work.

Spectroscopic Methods

Infrared spectra were recorded as KBr pellets (4000–400 cm^{-1}) on a Nicolet FTIR 7199 spectrophotometer equipped with a He–Ne laser. Resolution was 2 cm^{-1}. The spectra were corrected for background by a subtraction procedure. The 400–200 cm^{-1} region was recorded on a Perkin-Elmer 783 spectrometer.

The 514.5 nm line from a Spectra Physics Model 165 argon ion laser was used to record Raman spectra from a Spex Model 1400 microcomputer-controlled spectrometer. The samples were contained in sealed capillary tubes and rotated at high speed. The laser power was kept very low (20 to 50 mW depending on the sample) to minimize decomposition. The spectra were typically recorded at 5 cm^{-1} spectral slit width with a 2 s integration time at each 2 cm^{-1} frequency increment.

The ^1H NMR spectra were recorded at ambient probe temperature on a Bruker WH-400 spectrometer. They were referenced to Me_4Si. DMF-d_7 (Merck, Sharp & Dohme Canada) was the solvent.

Crystal Structure of $Mo_2(O_2CCH_3)_2(Aza)_2 \cdot 2DMF$

$C_{24}H_{30}Mo_2N_6O_6$, formula weight = 690.42, monoclinic, $P2_1/c$, $a = 8.378(2)$, $b = 9.166(2)$, $c = 17.384(4)$ Å, $\beta = 101.21(2)°$, $V = 1309.4$ Å^3, $D_{calc} = 1.745$ g cm^{-3}, $Z = 2$, λ(Cu K$\bar{\alpha}$) = 1.54178 Å (graphite monochromator), $T = 168$ K, μ(Cu Kα) = 84.3 cm^{-1}, crystal dimensions (mm) = 0.129 × 0.091 × 0.190.

The reduced cell was determined from a set of 25 randomly distributed reflections generated by the automatic search procedure and centered in the counter of an Enraf-Nonius CAD-4 diffractometer. This cell was checked by means of oscillation photographs taken about each of the cell axes. These diagrams showed the expected layer-line separations, and a Laue Mirror was found for oscillation about the 9.166 Å axis. The Niggli coefficients unambiguously ruled out all symmetries higher than monoclinic. The systematic absences ($h0l$, $l \neq 2n$; $0k0$, $k \neq 2n$) eventually noted in the full data set identified $P2_1/c$ as the only suitable space group.

The intensity data were collected following the procedure described earlier [7]. The seven standard reflections fluctuated within ±1.4% during the experiment. A total of 2478 independent hkl and $hk\bar{l}$ reflections were collected within a reciprocal sphere limited by $2\theta = 120°$. Of these data, 2199 with $I > 3\sigma(I)$ were retained for structure determination. They were corrected for the Lorentz effect, polarization and absorption (Gaussian integration, grid 8 × 8 × 8, transmission range = 0.28–0.56).

In space group $P2_1/c$, the dimer must lie on a crystallographic inversion center, so that the asymmetric unit corresponds to one of each building units (Mo, acetate, Aza and DMF). The Mo atom was located from a Patterson map. A Fourier difference (ΔF) map gave clear positions for the non-hydrogen atoms of DMF and the acetate group. Most of the Aza unit could be recognized in the map, but C4 and C9 each appeared as pairs of peaks. One set of peaks defining a reasonable geometry was first introduced into the model with full occupancies. Isotropic refinement on $|F_o|$ by full-matrix least-squares gave agreement factors $R = \Sigma \| F_o| - |F_c \| / \Sigma |F_o|$ and $R_w = [\Sigma w(|F_o| - |F_c|)^2 / \Sigma w |F_o|^2]^{1/2}$ of 0.088 and 0.101, respectively. However, abnormally high thermal parameters were found in the Aza rings, especially for C4 and C9. Careful examination of the previous ΔF map revealed that the pairs of peaks for some of the carbon atoms actually defined two superimposed ligands differently oriented, the five-membered ring of one image being roughly superimposed with the six-membered ring of the other, and vice versa. The N1, C2, C3, C5, C6, N7 and C8 atoms of one image were roughly coincident with N7′, C6′, C5′, C3′, C2′, N1′ and C8′, respectively, in the other image. Therefore, N1/7′, C2/6′, C3/5′, C5/3′, C6/2′, N7/1′ and C8/8′ were assigned full occupancies. The remaining ring positions (that is C4′ and C9′ for the primed image, C4 and C9 for the unprimed one) were given half occupancies. Refinement (isotropic for Aza and anisotropic for the remaining atoms) converged to $R = 0.050$ and $R_w = 0.061$. Then all non-methyl hydrogen atoms were fixed at idealized positions (C–H = 0.95). A new ΔF map revealed at least one hydrogen position for each methyl group, allowing the remaining hydrogens to be fixed. The hydrogen parameters were not refined, but their coordinates were recalculated after each least-squares cycle. Anisotropic refinement of all non-hydrogen atoms (block-diagonal least-squares) converged to $R = 0.039$ and $R_w = 0.045$, with a goodness-of-fit ratio of 3.24. The final ΔF map had a general background below ±0.6 e Å^{-3}.

The scattering curves used were from standard sources [8]. The real and imaginary contributions to anomalous dispersion of Mo were taken from Cromer [9]. The final coordinates are listed in Table 1. See also 'Supplementary Material'.

TABLE 1. Refined Fractional Coordinates ($\times 10^4$, Mo $\times 10^5$) and Equivalent Temperature Factors ($\times 10^3$) for $Mo_2(O_2CCH_3)_2(Aza)_2 \cdot 2DMF$[a]

Atom	x	y	z	U_{eq}
Mo	57757(5)	3370(4)	5232(2)	28
O11	3806(4)	1262(3)	959(2)	33
O12	2183(4)	563(4)	−143(2)	35
O23	7814(5)	954(6)	1809(2)	71
N7/1′	4514(6)	1678(5)	−1124(3)	45
N1/7′	6215(5)	2460(4)	36(3)	46
N20	8885(5)	2018(5)	2966(2)	38
C8/8′	5446(7)	2688(6)	−716(3)	47
C11	2418(6)	1178(5)	527(3)	33
C12	985(6)	1841(6)	803(3)	42
C21	9972(8)	842(8)	3235(4)	63
C22	8871(8)	3224(7)	3501(4)	59
C23	7868(7)	1951(7)	2287(3)	49
C2/6′	7084(7)	3649(6)	320(4)	52
C6/2′	3924(8)	2198(7)	−1872(3)	56
C3/5′	7083(8)	4846(6)	−144(4)	53
C5/3′	4394(7)	3591(7)	−2027(3)	56
C4	5426(17)	4641(15)	−1505(9)	71
C4′	6264(13)	5080(10)	−955(6)	37
C9′	5376(11)	3896(9)	−1287(5)	30
C9	6047(14)	4181(12)	−774(7)	50

[a] Symbols of the type N7/1′ are used for atomic positions coincident in the two disordered individuals, e.g. N7 in the unprimed orientation and N1 in the primed orientation.

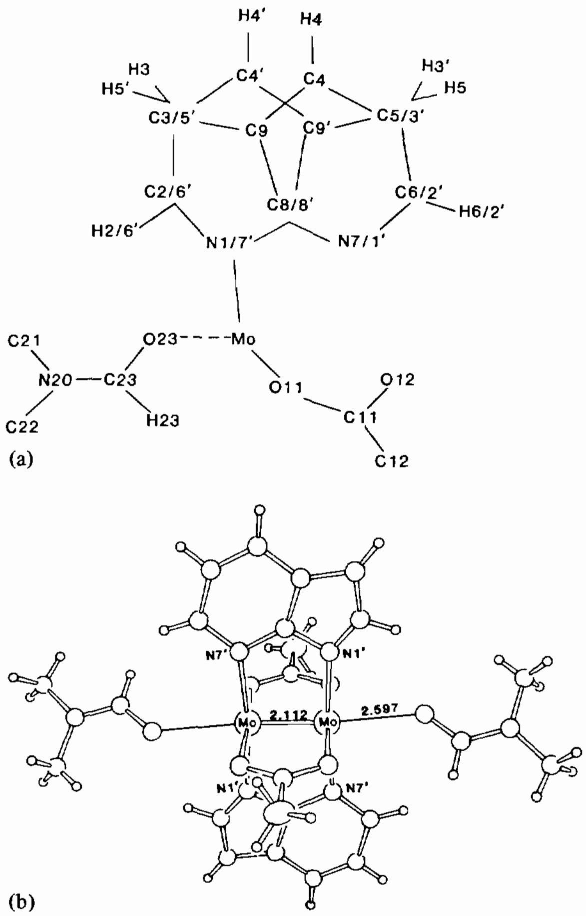

Fig. 1. (a) Numbering scheme in the asymmetric unit (half molecule) of $Mo_2(O_2CCH_3)_2(Aza)_2 \cdot 2DMF$. (b) ORTEP drawing of the centrosymmetric C_{2h} isomer present in the crystal. Ellipsoids correspond to 50% probability, except for the hydrogens and the disordered carbons of azaindole, whose thermal ellipsoids have been artificially adjusted.

Results and Discussion

Crystal Structure

Figure 1 shows a centrosymmetric $Mo_2(O_2CCH_3)_2(Aza)_2 \cdot 2DMF$ molecule containing acetate and azaindole monoanions (Aza^-) both acting as bridging ligands. Alternance of these two ligands about the Mo≡Mo quadruple bond generates a *trans* N_2O_2 arrangement about each metal atom. The dihedral angles between the acetate and azaindolyl planes are 88° and 92°. This $Mo_2L_2L_2'$ framework has an approximate C_{2h} symmetry with the two-fold axis running along the acetate $C-CH_3$ bonds. When the orientation of the axial DMF molecules and minor distortions in the bridging ligands are considered, the two-fold axis disappears, leaving the crystallographic inversion centre in the middle of the Mo≡Mo bond as the only symmetry rigorously present.

Interatomic distances and bond angles around Mo are listed in Table 2. Our Mo–Mo distance (2.1121(5) Å) is slightly shorter than observed for $Mo_2Cl_2(PEt_3)_2(Aza)_2$ (2.125(1) Å) [3], but longer than those of various $Mo_2(O_2CR)_4$ compounds (R = H, CF_3, CMe_3, Ph [10], Me [11], mean = 2.091 Å). This intermediate value can be ascribed to the different 'bites' of the two ligands. The O...O separation in the coordinated acetate is 2.216(4) Å, whereas the N1...N7 distance in the Aza^- ligand is 2.341(7) Å. This is also reflected in the Mo–Mo–ligand angles: the Mo–Mo–N angles are ~1.5° greater than the Mo–Mo–O angles. The Mo–O–C angles (mean 117.4(2)°) are close to the expected value of 120°. On the other hand, the presence of the N donors in a fused-ring system, with one ring being five-membered, renders the lone pair orientations somewhat divergent, so that the 'natural' Mo–Mo separation for binding exactly along the expected lone pair direction would be 2.94 Å (assuming Mo–N distance of 2.17 Å). With the present

TABLE 2. Selected Interatomic Distances and Bond Angles

Distances (Å)			
Mo–Mo^{a}	2.1121(5)	C11–C12	1.505(7)
Mo–N1/7′	2.182(4)	C11–O11	1.257(6)
Mo–N7/1′^{a}	2.159(4)	C11–O12	1.274(6)
Mo–O11	2.123(3)	N20–C21	1.430(8)
Mo–O12^{a}	2.117(3)	N20–C22	1.446(8)
Mo–O23	2.597(4)	N20–C23	1.316(7)
		C23–O23	1.230(8)
Angles (°)			
Mo^{a}–Mo–O11	91.90(9)	O11–C11–C12	119.1(4)
Mo^{a}–Mo–O12	90.94(9)	O12–C11–C12	118.6(4)
Mo^{a}–Mo–N1/7′	92.8(1)	O11–C11–O12	122.3(4)
Mo^{a}–Mo–N7/1′^{a}	93.3(1)	Mo–O11–C11	117.1(3)
Mo^{a}–Mo–O23	175.1(1)	Mo^{a}–O12–C11	117.8(3)
N1/7′–Mo–O11	89.1(2)	Mo–N1/7′–C8/8′	115.3(4)
N1/7′–Mo–O12^{a}	91.1(2)	Mo–N7/1′–C8/8′	116.7(4)
N7/1′^{a}–Mo–O11	90.0(2)	C21–N20–C22	116.8(5)
N7/1′^{a}–Mo–O12^{a}	89.5(2)	C21–N20–C23	121.2(5)
O11–Mo–O12^{a}	177.2(1)	C22–N20–C23	121.8(5)
N1/7′–Mo–N7/1′^{a}	173.8(2)	N20–C23–O23	125.0(5)
		C23–O23–Mo	132.4(4)

$^{a}1 - x, -y, -z$.

Mo–Mo distance, the Mo–N1–C8 angle is 115.3(4)°, whereas the lone pair would normally make a 126° angle with the N1–C8 bond. In summary, the presence of the 'wide-bite' Aza ligand increases the Mo–Mo separation compared to carboxylates, but not quite as much as in the $Mo_2Cl_2(PEt_3)_2(Aza)_2$, where only Aza is present in a bridging role.

The presence of axially coordinated DMF may also contribute to lengthening the Mo≡Mo quadruple bond, although it is well known that these bonds are much less affected by the presence of axial ligands than the Cr≡Cr bonds for instance. The Mo–O(DMF) distance of 2.598(4) Å compares well with the Mo–axial distances in $Mo_2(O_2CCF_3)_4 \cdot 2Py$ (2.548(8) Å [12]) and $Mo_2(O_2CPh)_4$(Diglyme) (2.663(6) Å [13]).

The geometry of the axial DMF (Table 2) is typical of those observed in crystal structures of DMF complexes or solvates*. The acetate groups are also similar to those found for $Mo_2(O_2CCH_3)_4$ [11] and other acetate-containing dimolybdenum compounds. Because of the disorder, individual distances and angles in the azaindole anion (see 'Supplementary Material') are not very reliable. They do not significantly differ from those observed for complexes containing azaindole as a monodentate donor via N7 [15, 16]. The two individual Aza ligands are found to be planar within 0.04 Å (3 σ).

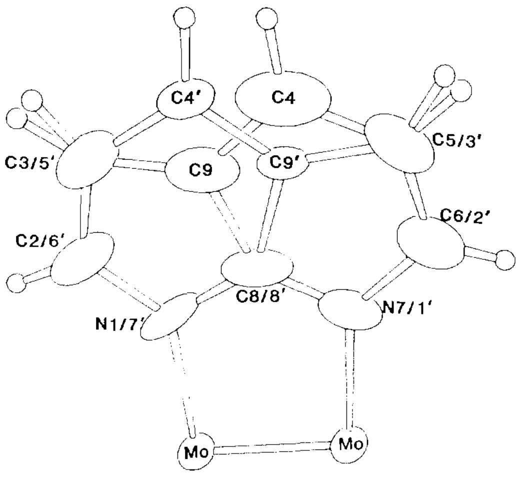

Fig. 2. Superimposed images of the two disordered half-molecules of 7-azaindole in the crystal.

The Aza ligand is found to be disordered over two orientations in the crystal, with the six- and the five-membered rings exchanging positions (Fig. 2). The same type of two-fold disorder has recently been found to occur in cobalt– and copper–azaindole complexes [17]. This is made possible by the very similar van der Waals envelopes for the two orientations. Judging from the shape and size of the thermal ellipsoids, it is likely that a similar disorder occurred to some extent in the structure of $Mo_2Cl_2(PEt_3)_2(Aza)_2$, although resolution into two individuals was not possible in that case [3].

Because of the disorder, X-ray diffraction cannot determine unambiguously the relative orientation of the two Aza ligands within a given molecule. For instance, assuming that a given Mo atom is attached to N1 of one Aza ligand, the other Aza group can be attached to the same metal either via N7, leading to the C_{2h} framework of Fig. 1, or via

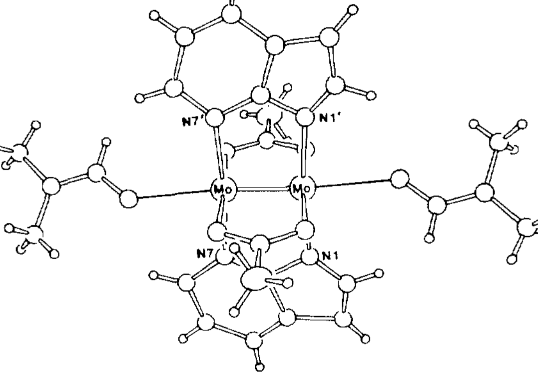

Fig. 3. ORTEP drawing of the C_{2v} form of $Mo_2(O_2CCH_3)_2$-$(Aza)_2 \cdot 2DMF$ also present in the crystal.

---

*Mean distances and angles in DMF molecules coordinated to metal atoms or trapped in crystal lattices have been calculated for over 30 crystal structures. See (Supplementary Material' (Table VII) and ref. 14.

N1, thereby defining a C_{2v} framework with an approximate mirror plane parallel to the Mo≡Mo bond through each pair of ligand (Fig. 3). Since the two disordered orientations are equally populated, it must be concluded that each of these isomers is packed in two orientations with equal probabilities, as illustrated in Fig. 4. Therefore, X-ray work cannot determine whether both isomers are present and if so, in what proportions. The ^{1}H NMR spectra (*vide infra*) provide evidence for roughly equal populations of both forms. The molecules are packed with normal van der Waals contact in the unit cell, as shown in Fig. 5.

Vibrational Spectroscopy

The approximate assignments proposed for 7-azaindole are made by comparison with indole [18]. $Mo_2(O_2CCH_3)_4$ has been discussed briefly in previous papers [19, 20]. The acetate modes were identified by comparison with those of $CrMo(O_2CCH_3)_4$ [21] and $Cu_2(O_2CCH_3)_4 \cdot 2H_2O$ [22].

The Raman spectra of 7-azaindole, $Mo_2(O_2CCH_3)_4$ and $Mo_2(O_2CCH_3)_2(Aza)_2$ were recorded between 800 and 150 cm^{-1} (Table 3). The spectrum obtained for $Mo_2(O_2CCH_3)_2(Aza)_2 \cdot 2DMF$ was identical with that of $Mo_2(O_2CCH_3)_2(Aza)_2$, indicating decomposition to the unsolvated molecule in the laser beam.

The spectrum of $Mo_2(O_2CCH_3)_2(Aza)_2$ shows characteristic absorptions for the acetate and 7-azaindole groups both present in the complex. The shifts of +40 and +20 cm^{-1} on the azaindole out-of-plane vibrations at 437 and 428 cm^{-1}, respectively, also observed in the infrared, are typical of azaindole coordinated in the deprotonated form [23].

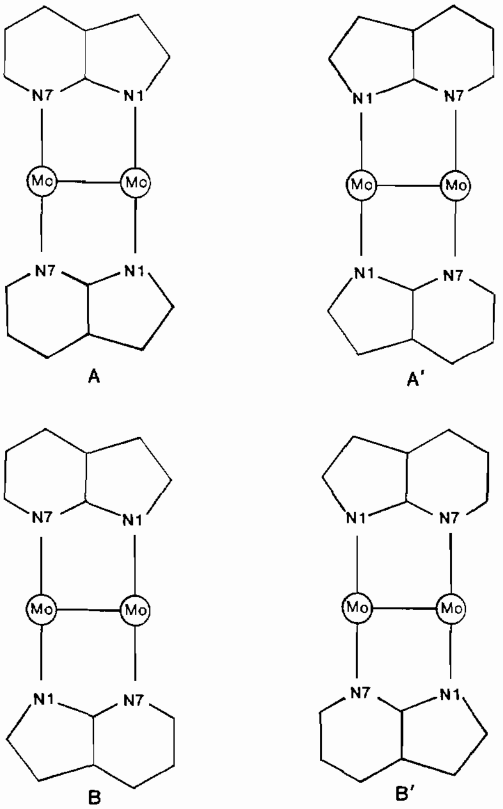

Fig. 4. Schematic representation of the four possible arrangements of the $Mo_2(Aza)_2$ fragment in the crystal.

TABLE 3. Raman Frequencies of 7-Azaindole and its Mo Complexes (cm^{-1})^a

HAza	$Mo_2(OAc)_2$-$(Aza)_2$	$Mo_2(OAc)_4$	Assignment
768(10)	792(10)		R′ (breathing)
727(1)			γ C–H
		692(10)	δ O–C–O
	686(1)	686(9)	
622(6)	633(2)	633(1)	R″; ρ O–C–O
		566(1)	
565(1)			R″
557(2)			R′
437(1)	476(6)		R″
428(1)	448(1)		R″
	377(7)	406(10)	ν Mo–Mo
		323(4)	ν Mo–O and/or ν Mo–N
	313(1)	314(3)	
	301(1)	300(4)	
259(1)			R″
238(1)	242(4)		R″
	212(5)	201(4)	$Mo_2O_4N_4$ or Mo_2O_8 deformation
	188(9)	188(4)	

^{a}Within parentheses, intensity relative to 10 for the strongest peak. Abbreviations: δ, in-plane bending; γ, out-of-plane bending; ρ, rocking; ν, stretching; R′, in-plane azaindole ring vibration; R″, out-of-plane ring vibration.

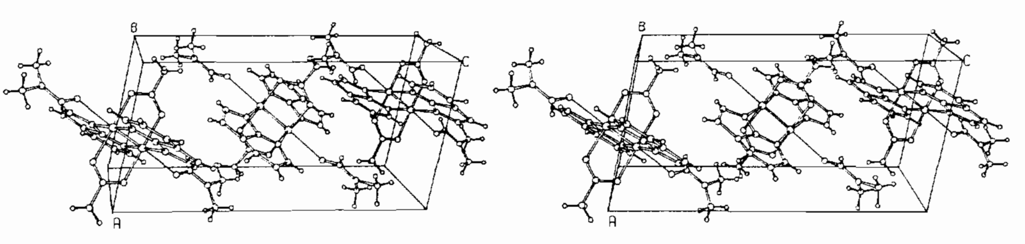

Fig. 5. Stereoview of the unit cell of $Mo_2(O_2CCH_3)_2(Aza)_2 \cdot 2DMF$.

TABLE 4. Infrared Frequencies of 7-Azaindole and its Mo Complexes (cm^{-1})[a]

HAza	$Mo_2(OAc)_2$-$(Aza)_2$	$Mo_2(OAc)_2$-$(Aza)_2 \cdot 2DMF$	$Mo_2(OAc)_4$	Assignment
		1656vs		ν C=O(DMF)
1600s	1595m	1598s		R′
1584vs				R′
	1556w			
		1539s		δ CH_3 (DMF)
	1515s	1510s	1516m	[ν_a O–C–O]
	1490s	1490sh	1496s	
1498m	1460s	1463s		R′
		1434vs	1443vs	R′ and/or
1422vs	1419vs	1416vs	1410s	[δ_a CH_3 + ν_s O–C–O]
		1386m		δ_s CH_3 (DMF)
		1362m		
1345s	1354m	1350m	1352s	R′; [δ_s CH_3]
1336s	1336s	1342s		R′
1331s				
1279vs	1280s	1285m		R′
		1270m		ν N–CH_3 (DMF)
		1261m		
1253m	1251m	1250m		δ C–H
1208w	1203w	1203vw		R′
1196w				δ N–H
1124w	1147vs	1154m		δ C–H
1107s	1121w	1118vw		δ C–H
		1098w		ρ CH_3(DMF)
1071sh	1074vw	1061w		δ C–H
1065w				
	1038w	1044w	1046m	[ρ CH_3]
	1022w	1015w	1032m	
955w	970w	957m		γ C–H
924w	936m	944m	937m	γ C–H; [ν C–CH_3]
900s	916m	910w		R′
883s		888w		γ C–H; ν N–CH_3(DMF)
860m				γ N–H
851m				
793s	789m	803s		γ C–H
		790sh		
764vs	760m	772m		R′
729sh	734m	738vs		γ C–H
720vs	723m			γ C–H
	672vs	668m	675m	[δ O–C–O]
		660m		δ O–C–N(DMF)
621s	633m		632m	[ρ O–C–O];
618s	627w	624w	628m	R″
599m	611w			R′
594m				
573vw	581w		578w	R″
563m	567w		571w	and/or
				[ρ O–C–O];
560m				and/or
557m				R′
434m	474m	472w		R″
426m		445w		R″
			370m	
			352sh	[ν Mo–O];
	336m	335m	340s	ν Mo–O (or N)
	318m	324m		

[a] Dimethylformamide vibrations labelled (DMF), Mo–acetate vibrations within square brackets. Abbreviations: vs, very strong; s, strong; m, medium; w, weak; vw, very weak; sh, shoulder; R′, in-plane azaindole ring vibration; R″, out-of-plane ring vibration.

The most interesting feature is the strong Mo–Mo stretching vibration observed at 377 cm^{-1}. This value lies in the middle of the 330–425 cm^{-1} range associated with quadruply-bonded dimolybdenum units [1]. For $Mo_2(O_2CCH_3)_4$, this band is found at 406 cm^{-1}. Thus the substitution of two acetate groups by azaindole anions decreases the Mo–Mo frequency by 29 cm^{-1}, which reflects the lengthening of the Mo–Mo bond in the present mixed compound.

The infrared spectra of $Mo_2(O_2CCH_3)_2(Aza)_2$ and its DMF adduct are compared with those of $Mo_2(O_2CCH_3)_4$ and 7-azaindole in Table 4.

Substitution of the N1-H proton produced a drastic decrease in intensity at ~2900 cm^{-1}, where the azaindole ν(N–H) vibration produces a strong and broad absorption. The ligand γ(N–H) band at 851 cm^{-1} is also removed. Between 1100 and 1200 cm^{-1} are found three bands at 1196, 1124 and 1107 cm^{-1}, originating from coupled δ(N–H) and δ(C–H) motion. One of these bands disappears in the complex, leaving the two δ(C–H) modes at 1147 and 1121 cm^{-1}. Large shifts are also found for the following ligand bands upon complexation: 1124 (+25 and intensity increase), 1107 (+12, and intensity loss), 434 (+40) and 425 (+20). We have found similar spectral changes in the spectra of $[(CH_3Hg)(Aza)]$ and $[(CH_3Hg)_2(Aza)]^+$ salts, which are N1- and N1/7-bonded, respectively [23]. Therefore, they mainly reflect the presence of the azaindole ligand in the anionic form in this complex, and provide no information concerning the role of N7. The only clear infrared evidence for N1/N7 binding is provided by displacement of the strong ring band from 1498 to 1462 cm^{-1}. This same shift has been noted for the $[(CH_3Hg)_2(Aza)]^+$ species, but not for $[(CH_3Hg)(Aza)]$ [23]. It seems to be a good diagnostic for bidentate behavior of azaindole via N1 and N7.

Even though the environment of the acetate ligands has changed, their infrared bands occur almost at the same place as in $Mo_2(O_2CCH_3)_4$ [19].

Various new bands due to dimethylformamide [24] are found in the spectrum of the adduct. The C=O stretching vibration is clearly observed as a very strong band at 1656 cm^{-1}. The δ_s CH_3 mode produces a doublet at ~1370 cm^{-1}, whereas antisymmetric C–N–C stretching in the $-N(CH_3)_2$ group gives another doublet at ~1265 cm^{-1}. The δ(O–C–N) deformation vibration is also detected at 660 cm^{-1}.

TABLE 5. ^{1}H NMR Data for 7-Azaindole and $Mo_2(O_2CCH_3)_2(Aza)_2$ in DMF-d_7 ^{a}

Free ligand	Isomers A and B	
7-Azaindole		
H1 11.61		
H2 7.543 (2.39; 3.10)	7.484 (2.96)	7.409 (3.00)
H3 6.487 (1.87; 3.46)	6.693 (2.55)	6.687 (2.67)
H4 7.985 (b; 8.40)	8.086 (5.89; 1.21)	8.042 (b; b)
H5	7.069 (5.40; 7.32)	
H6 8.229 (1.51; 4.62)	8.146 (1.25; 7.41)	8.137 (1.20; 7.40)
Acetate		
CH_3 1.973	2.253	2.261
OH 12.21		

^{a}Chemical shifts (400 MHz) in ppm *vs.* Me_4Si; coupling constants in Hz within brackets. ^{b}Resonance obscured by the DMF signal at 8.023 ppm.

NMR Spectroscopy

The ^{1}H NMR spectrum of 7-azaindole in $CDCl_3$ solution was assigned by Cox and Sankar [25]. These assignments hold for the spectrum in DMF-d_7, although H2 appears 0.19 ppm upfield and H6 0.08 ppm downfield (Table 5 and Fig. 6). Also, the H2 and H3 doublets of the $CHCl_3$ spectrum are observed as doublets of doublets in DMF, as a result of extra coupling with the H1 proton, which appears as a broad peak at 11.63 ppm. This was checked by taking the spectrum of the N1-deuterated molecule, where the 11.6 ppm resonance disappeared and the H2 and H3 signals became doublets, as observed in $CHCl_3$. Further deuteration at C3 removed the 6.49 ppm signal and led to a singlet for the H2 peak at 7.54 ppm.

In Fig. 6, spectra of $Mo_2(O_2CCH_3)_2(Aza)_2$ in DMF-d_7 taken at various times are compared to that of free azaindole. These complicated spectra could be unraveled by first examining the H2 region at 7.55 ppm. Although the infrared spectrum showed no evidence for free azaindole in the sample and the solution was made under inert atmosphere, Fig. 5 shows that immediately after making the solution, free ligand accounts for a substantial part of the total azaindole present. Clearly, part of the complex quickly reacts with the water present in DMF-d_7, liberating neutral azaindole and acetic acid, the latter being detected from the methyl signal at 1.973 ppm and broad OH peak at 12.21 ppm. In this very dilute solution, even traces of water can hydrolyse a significant part of the complex present. After this initial step, hydrolysis proceeded more slowly as moisture diffused into the stoppered NMR tube, increasing the intensities of the free ligands signals at the expense of signals A and B, which were found to lose intensity at the same rate.

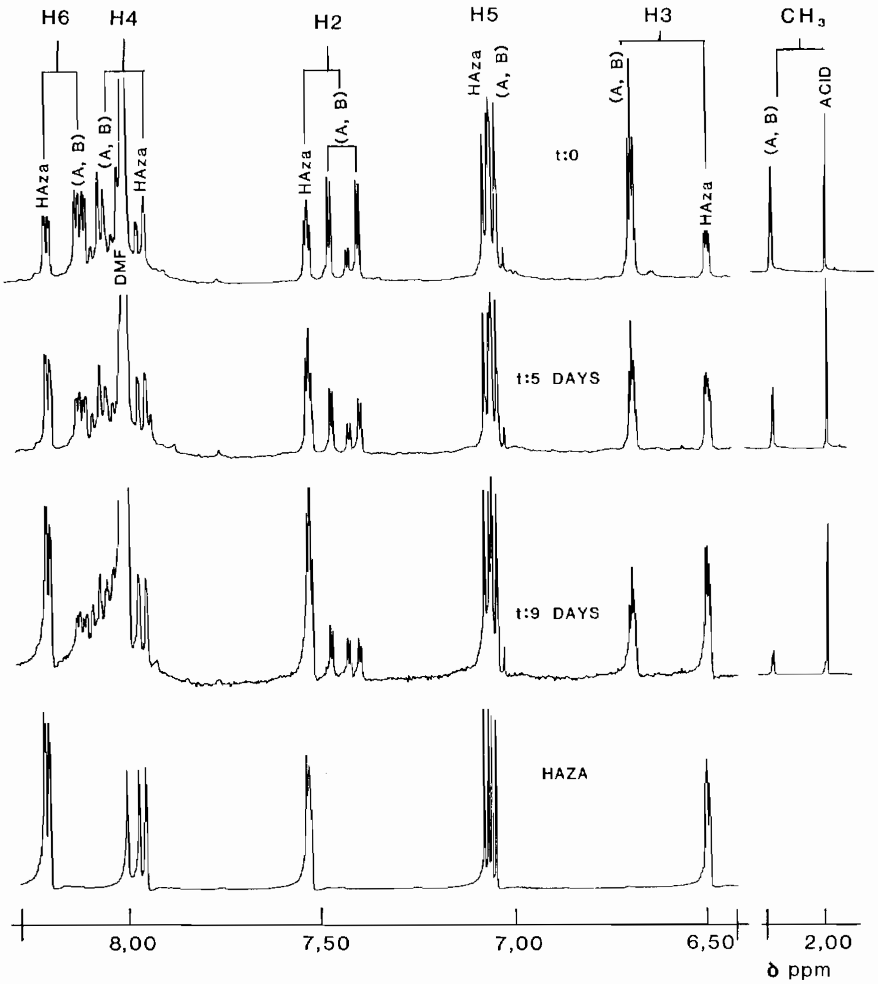

Fig. 6. ^{1}H NMR spectra of $Mo_2(O_2CCH_3)_2(Aza)_2 \cdot 2DMF$ and 7-azaindole in DMF-d_7.

The two sets of signals A and B are very likely due to the two isomeric forms of $Mo_2(O_2CCH_3)_2(Aza)_2$, whose presence in the crystal is suggested by the X-ray work. In C_{2h} form, the two azaindoles and the two acetates form symmetry-equivalent pairs, and only one set of signals should be observed. A second set of signals is expected for the C_{2h} form, in which the ligands are also symmetry equivalent. The appearance of the H2 and H3 resonances as doublets indicate that the N1-H proton is absent, as expected if azaindole remains coordinated. The splitting of the acetate signal into two equal components at 2.253 and 2.261 ppm is also consistent with this interpretation. However, since the intensities and coupling constants are roughly the same for the two sets, the signals cannot be individually assigned to a given isomer.

The very weak signal at ~7.44 ppm probably corresponds to a small amount of another azaindole complex present in the sample or generated upon dissolution in DMF. The remaining resonances are likely masked by those of A, B or free azaindole. The concentration seems to remain constant in the three spectra. It could be due to traces of an azaindole-rich complex less susceptible to hydrolysis, but no formal identification is possible.

Conclusion

In spite of the large 'bite' difference, acetate and azaindole can form stable mixed complexes. In $Mo_2(acetate)_2(Aza)_2 \cdot 2DMF$, the Mo≡Mo quadruple bond length is found to adopt an intermediate value, greater than in the tetraacetate, but less than in the $Mo_2Cl_2(PEt_3)_2(Aza)_2$ compound, where only azaindole is bridging. Using a bridging ligand like 7-azaindole, whose two rings are unequivalent but have similar van der Waals profiles, results in the formation of various stereoisomers with very close stabilities and properties. In the present case, the two stereoisomers of the mixed complex could not be separated, but they were identified from the X-ray work and ^{1}H NMR spectra.

Supplementary Material

The refined temperature factors as well as a table of observed and calculated structure factor amplitudes are available from the correspondence author on request.

Acknowledgements

We wish to thank M. Simard who collected the X-ray data, and M. Pigeon and R. Savoie (Université Laval), who recorded the Raman spectra. The financial support of the Natural Sciences and Engineering Research Council of Canada and the Ministère de l'Education du Québec is gratefully acknowledged.

References

1 F. A. Cotton and R. A. Walton, *Multiple Bonds Between Metal Atoms,* Wiley, New York, 1982, Ch. 3.

2 A. T. Baker, W. R. Tikkanen, W. C. Kaska and P. C. Ford, *Inorg. Chem., 23* (1984) 3254; W. R. Tikkanen, E. Binamira-Soreaga, W. C. Kaska and P. C. Ford, *Inorg. Chem., 23* (1984) 141.

3 F. A. Cotton, D. G. Lay and M. Millar, *Inorg. Chem., 17* (1978) 186.

4 C. D. Garner, S. Parkes, I. B. Walton and W. Clegg, *Inorg. Chim. Acta, 31* (1978) L451; F. A. Cotton, W. H. Ilsley and W. Kaim, *Inorg. Chim. Acta, 18* (1979) 267; D. M. Collins, F. A. Cotton and C. A. Murillo, *Inorg. Chem., 15* (1976) 1861.

5 V. G. Holste and H. Schafer, *Z. Anorg. Allg. Chem., 391* (1972) 263.

6 D. A. Edwards, G. Uden, W. S. Mialki and R. A. Walton, *Inorg. Chim. Acta, 40* (1980) 25.

7 F. Bélanger-Gariépy and A. L. Beauchamp, *J. Am. Chem. Soc., 102* (1980) 3462.

8 D. T. Cromer and J. T. Waber, *Acta Crystallogr., 18* (1965) 104; R. F. Stewart, E. R. Davidson and W. T. Simpson, *J. Chem. Phys., 42* (1965) 3175.

9 D. T. Cromer, *Acta Crystallogr., 18* (1965) 17.

10 F. A. Cotton and J. G. Norman, Jr., *J. Coord. Chem., 1* (1971) 161; F. A. Cotton, J. G. Norman, Jr., B. R. Stults and T. R. Webb, *J. Coord. Chem., 5* (1976) 217; F. A. Cotton, M. Extine and L. D. Gage, *Inorg. Chem., 17* (1978) 172.

11 F. A. Cotton, Z. C. Mester and T. R. Webb, *Acta Crystallogr., Sect. B, 30* (1974) 2768.

12 F. A. Cotton and J. G. Norman, Jr., *J. Am. Chem. Soc., 94* (1972) 5697.

13 D. M. Collins, F. A. Cotton and C. A. Murillo, *Inorg. Chem., 15* (1976) 2950.

14 A. L. Beauchamp, M. J. Olivier, J. D. Wuest and B. Zacharie, *Organometallics, 6* (1987) 153.

15 F. A. Cotton and T. R. Felthouse, *Inorg. Chem., 20* (1981) 600; F. Allaire and A. L. Beauchamp, Structure of $Rh_2(acetate)_4 \cdot 2(7\text{-azaindole})$, to be submitted for publication.

16 W. S. Sheldrick, *Z. Naturforsch., Teil B, 37* (1982) 653.

17 S. M. Peng and Y. N. Lin, *Acta Crystallogr., Sect. C, 42* (1986) 1725.

18 A. Lautié, M. F. Lautié, A. Gruger and S. A. Fakhri, *Spectrochim. Acta, Part A, 36* (1980) 85; H. Takeuchi and I. Harada, *Spectrochim. Acta, Part A, 42* (1986) 1069.

19 W. K. Bratton, F. A. Cotton, M. Debeau and R. A. Walton, *J. Coord. Chem., 1* (1971) 121.

20 A. J. Hempleman, R. J. H. Clark and C. D. Flint, *Inorg. Chem., 25* (1986) 2915.

21 C. D. Garner, R. G. Senior and T. J. King, *J. Am. Chem. Soc., 98* (1976) 3526.

22 Y. Mathey, D. R. Greig and D. F. Shriver, *Inorg. Chem., 21* (1982) 3409; A. M. Heyns, *J. Mol. Struct., 11* (1972) 93.

23 P. Dufour, Y. Dartiguenave, M. Dartiguenave, N. Dufour, F. Bélanger-Gariépy and A. L. Beauchamp, in preparation.

24 G. Durgaprasad, D. N. Sathyanarayana and C. C. Patel, *Bull. Chem. Soc. Jpn., 44* (1971) 316.

25 R. H. Cox and S. Sankar, *Org. Magn. Reson., 14* (1980) 150.